



OPEN

# Electrical facies of the Asmari Formation in the Mansouri oilfield, an application of multi-resolution graph-based and artificial neural network clustering methods

Seyedeh Hajar Eftekhari<sup>1</sup>, Mahmoud Memariani<sup>1✉</sup>, Zahra Maleki<sup>1</sup>, Mohsen Aleali<sup>1</sup> & Pooria Kianoush<sup>2,3</sup>

Electrofacies analysis conducted the distribution effects throughout the reservoir despite the difficulty of characterizing stratigraphic relationships. Clustering methods quantitatively define the reservoir zone from non-reservoir considering electrofacies. Asmari Formation is the most significant reservoir of the Mansouri oilfield in SW Iran, generally composed of carbonate and sandstone layers. The stratigraphical study is determined by employing 250 core samples from one exploratory well in the studied field. Five zones with the best reservoir quality in zones 3 and 5 containing sandstone/shale are determined. Moreover, multi-resolution graph-based and artificial neural network clustering involving six logs are employed. Utilizing Geolog software, an optimal model with eight clusters with better rock separation is obtained. Eventually, five electrofacies with different lithological compositions and reservoir conditions are identified and based on lithofacies describing thin sections, sandstone, and shale in zones 3 and 5 show high reservoir quality. According to the depth related to these zones, most of the facies that exist in these depths include sandstone and dolomite facies, and this is affected by the two factors of the primary sedimentary texture and the effect of the diagenesis process on them. Results can be compared to the clustering zone determination in other nearby sandstone reservoirs without cores.

**Keywords** Asmari reservoir, Electrofacies, Lithofacies, Zoning, MRGC and ANN clustering, Sandstone reserve

## Abbreviations

ACE	Alternating conditional expectations
ANN	Artificial neural network
EF	Electrofacies
FZI	Flow zone index
HCA	Hierarchical cluster analysis
KPCA	Kernel principal component analysis
KRI	Kernel Representative Index
LF	Lithofacies
L-M	Levenberg–Marquardt algorithm
MRGC	Multi resolution graph based clustering
RKHS	Reproducing kernel Hilbert space
SONN	Self organized neural network

<sup>1</sup>Department of Earth Sciences, Science and Research Branch, Islamic Azad University, 1477893855 Tehran, Iran. <sup>2</sup>Department of Petroleum and Mining Engineering, South Tehran Branch, Islamic Azad University, Tehran, Iran. <sup>3</sup>National Iranian Oil Company, Exploration Directorate (NIOC-EXP), Tehran, Iran. ✉email: Mahmoud.memariani@gmail.com; memarianim@yahoo.com

The broad meaning of "facies" is the characteristics, appearance, and aspects of a rock unit, usually imaging the circumstances of its origin, particularly determining the unit from neighboring or associated units<sup>1–4</sup>. Electrofacies are numerical mixtures of petrophysical log reactions that reflect a rock interval's compositional characteristics and specific physicals. They are confined by multivariate techniques that contain discriminant, cluster, and Principal Components Analysis (PCA)<sup>5–8</sup>. Electrofacies specify reservoir rock properties, especially permeability, to simulate fluid flow in porous media. These are determined based on the classification of similar logs among different groups of logging data. Data classification is accomplished by statistical analyses such as principal component analysis, cluster analysis, and differential analysis<sup>3,9–11</sup>. A model of the reservoir's geological structure is also provided to create a three-dimensional model of a reservoir's properties, in addition to estimating porosity, permeability, water saturation, and other petrophysical properties. For geological modeling, lithofacies describe rock or sedimentary units with texture, structure, mineralogy, and rock properties, and these units can be employed to match important reservoir characteristics such as permeability and porosity<sup>12–14</sup>.

Therefore, identifying different rock facies of reservoir rock is a fundamental task in describing the characteristics of oil reservoirs. Detection of lithofacies in the repository is complex because the type and distribution of the facies are determined by the deposition system and are affected or altered by diagenesis and tectonics<sup>14,15</sup>. The most common technique for determining lithofacies is coring. The core data directly observes the lithofacies and can accurately distinguish the different facies. However, despite all the positive features, due to the high cost of core-extraction operations and the lack of 100% recovery, this method can only be employed in a small section of the field around the wellbore<sup>1,14,16–18</sup>.

On the other hand, core description is time-consuming and depends on the geologist's experience. Therefore, solving this problem requires a procedure cheaper than coring and capable of providing precision and separation of the rock facies to a suitable size similar to that of cores without wells<sup>19–24</sup>. An excellent way to respond to this demand is utilizing well-log data. Data loggers obtain indirect information from underground data and are much cheaper than kernels. Well-log calculations can be categorized into facies or electrical facies. Log facies can display rock and reservoir fluid properties and allow users to separate sedimentary units and layers. Created facies can be later applied to predict rock facies in intervals without core<sup>11,25,26</sup>. A practical method for facies analysis is to create a facies classification model that splits the log data into a set of log responses that describes sediment and provides sediment separation and identification from other sediments. This set of responses is called a cluster. These clusters have significant problems with dependency on the dimensionality, which differed from the geological distance and the two similar points in interpreting the cluster. They may not be geologically similar. The reason for this problem is the different views of geologists and loggers. This problem creates a nonlinear solid relationship between log and lithology and causes the problem of determining any partitioning of the log data into the associated sedimentary unit<sup>17,22,27,28</sup>.

The easy determination and application of this zoning and its reliance on log data make it possible to quickly and accurately distinguish reservoir segments from non-reservoir segments. With overgrowing the world, the cluster analysis method is utilized as the principal direction analysis of the log facies identification<sup>4,7,29–31</sup>. It is employed as an essential tool for logging in advanced petroleum software. Since these facies are determined only by pure mathematical processes in the cluster analysis method and no training or fitting function is considered, they are very accurate, and their application is not limited to a particular well or field. After identifying the log facies by assigning geological features to them, it can be applied to other wells on the surface of adjacent fields to match and predict the desired features<sup>2,7,15,32,33</sup>.

An essential advantage of electrofacies over alternative types of facies classifications of rocks in the subsurface is that electrofacies can be defined solely based on well-log responses without reliance on cores, cuttings, or outcrops. Although electrofacies are empirical, they are also objective; no subjective interpretations of sediment genesis or inferences about depositional environments are required. Moreover, there is no specific procedure for defining electrofacies. The general requirements could be defined from a uniform set of petrophysical log measurements with similarities between down-hole intervals are expressed quantitatively from the log responses. The intervals are consistently divided into subsets that have similar responses, and distinctions between subsets are expressed as mathematical functions<sup>3,7,34</sup>.

As the literature review of recent years, Serra and Abbott<sup>35</sup>, and Serra<sup>36</sup> defined electric facies as "a set of responders that, in addition to characterizing the sediments, allows them to be separated." Wolf and Pelissier-Combes<sup>37</sup>, and Selley<sup>38</sup> introduced the first automated method for classifying "facsimiles" into electrical facies. Tavakkoli and Amini<sup>39</sup> employed a set of logs instead of one log to assign more features to a particular logfacies simultaneously. In 2015, some studies of identifying and interpreting electrical facies employing the Self Organized Neural Network (SONN) method and its prediction for sedimentary facies in the Asmari reservoir of an SW oilfield of Iran have been carried out<sup>26,40</sup>. Kiaei et al.<sup>26</sup> Modeled three-dimensional reservoir electro-physics using integrated clustering and geostatistical methods in the Persian Gulf. Their approach included Hierarchical Cluster Analysis (HCA), Multi Resolution Graph-based Clustering (MRGC), and self-Organized Maps (SOM). Based on their results, hierarchical clustering as a robust and practical approach to data clustering was performed based on profile validation and geological information.

El Sharawy and Gaafar<sup>41</sup> zoned the reservoir based on statistical analyzes in the Nubian sandstone Gulf of Suez, Egypt. They showed that the entire reservoir could be divided into at least four electro physics with significant changes in reservoir quality, which correlated with permeability changes. Tian et al.<sup>42</sup> employed the multi-resolution graph-based clustering (MRGC) method for determining the Electrofacies (EF) and Lithofacies (LF) from well-log data obtained from the intraplatform bank gas fields located in the Amu Darya Basin. Rastegarnia et al.<sup>9</sup> predicted 3D Flow Zone Index (FZI) and electrified (EFACT) volumes from a large volume of 3D seismic data. Rafik and Kamel<sup>16</sup> evaluated the permeability of the formation for a sandstone reservoir in the South Ramsey reservoir formations from log well data utilizing multivariate methods. Their results showed that permeability prediction using variable selection to non-parametric Alternating Conditional Expectations

(ACE) regression is the best way to predict permeability. Kadkhodaie and Kadkhodaie<sup>27</sup> reviewed different reservoir rock typing approaches from geology to seismic and dynamic and proposed an integrated rock type workflow for worldwide carbonate reservoirs. Jafarzadeh et al.<sup>18</sup> investigated the distribution of reservoir facies employing the available data to identify areas that are prone to be considered in the production and development plans of the field in terms of their storage and fluid flow capacity. Eventually, the experimental results illustrated that the adaptive multi-resolution graph-based clustering algorithm for electrifying analysis also outperformed the original MRGC approach on clustering and propagation prediction with higher efficiency and stability<sup>34,43,44</sup>. Recently, the electrified predicted using the MRGC approach to generate rock mechanical properties such as Young's modulus, Poisson's ratio, unconfirmed compressive strength, and internal friction coefficient<sup>5,45,46</sup>. Kianoush<sup>47</sup> estimated an ANN based model of formation Pressure for the Azadegan hydrocarbon Reservoir, SW Iran. Finally, Okhovvat et al.<sup>8</sup> used Kernel Principal Component Analysis (KPCA) to improve the performance of electrical facies classification.

This study addresses some of the ambiguities of using drilling cuttings and logs data in analyzing petroleum formations by combining the results of logs and describing log facies. It is mainly done by defining the log facies and the reservoir zoning of the study well. Moreover, as an innovation, the wells are zoned employing well-logging diagrams, and then, utilizing MRGC and ANN techniques, electrical facies from log data are determined. Also, as a geological novelty, a zoning methodology for the Asmari Formation in the Mansouri field is considered. Two general lithofacies of carbonate-evaporitic facies and siliceous-clastic petrofacies are determined, describing thin sections that have acceptable consistency and similarity with electrofacies clustering of sandstone in deeper parts of Asmari reservoir. Furthermore, integrating ANN and MRGC clustering methods, instead of the limited and unique information of a few cored wells, comprehensive information on the simulated sedimentary facies is obtained in all the field wells, which immensely helped the sedimentary modeling of the studied field.

## Geological setting

### Structural geology

Mansouri field in the southernmost part of the north Dezful zone, about 45 km south of Ahwaz, is located approximately on the border of the Arabian Plate, and quaternary alluviums represent the Zagros Plate and its surface outcrop. Mansouri field is located in the north of the Ahwaz field, in the west, in the vicinity of the Abteymur and Susangerd fields, and the northeast of the Shadegan field. The axial trend of this field is from the northwest to the southeast (the general Dezful embayment) and lies between 48° to 52° east longitude and 30° to 32° north latitude (Fig. 1)<sup>6,21,40</sup>. Mansouri field is located in a flat zone just off the foot of the foothills and was discovered by seismic exploration in 1963. Based on the seismic and structural maps of the Mansouri field, it is an anticline with gentle and low slopes in the northwest-southeast (NW-SE) direction. The northern slopes are slightly higher than the southern ones<sup>7,24,40,48-50</sup>.

Furthermore, 5–6°, the slope of the eastern and western slopes is about 1–5°. The study of geophysical maps and the information on drilled wells show no evidence of fault or disruption in the field, and it is generally mild in structure (Fig. 1). Mansouri's field in the horizons of Asmari is about 42 km long. It has a variable width of up to 6 km in the middle of the field and an average of 4.5 km, which decreases to the east and west slopes. The dimensions of the reservoir at the contact surface of water and oil (2272 m below sea level) are 30 km long and 3.5 km wide, stretching northwest-southeast<sup>4,32,51-53</sup>.

The limestone Asmari Formation is the most critical Zagros sedimentary reservoir. In terms of sedimentation, it began in the former Oligocene and continued until the former Miocene. This formation is the shallow horizon of oil producers in SW Iran and forms the most essential rock reservoir in Dezful's embayment. The formation's upper and lower limit has the same slope. In addition to the Asmari reservoir and sandstone section of Ahwaz, the Bangestan reservoir (Ilam and Sarvak Formations) are also present in this field<sup>39,50</sup>.

### General stratigraphy

The stratigraphic column, reservoir zonation, and selected petrographic thin sections of the Bangestan reservoir are presented in Fig. 2 for one of the drilled wells. The Bangestan reservoir was subdivided into nine zones in the studied field based on petrography, petrophysical parameters, and well-logging data<sup>10,12,20,54</sup>.

The Asmari Formation geologically consists of sandstone, dolomite, limestone and low to average clay minerals. This formation is characterized by light brown, hard and fine-grained dolomite with lime layers, followed by medium to coarse grains, often without cement or calcareous and dolomite and sandy cement. White limestone to light grey is observed in the formation's lower part.

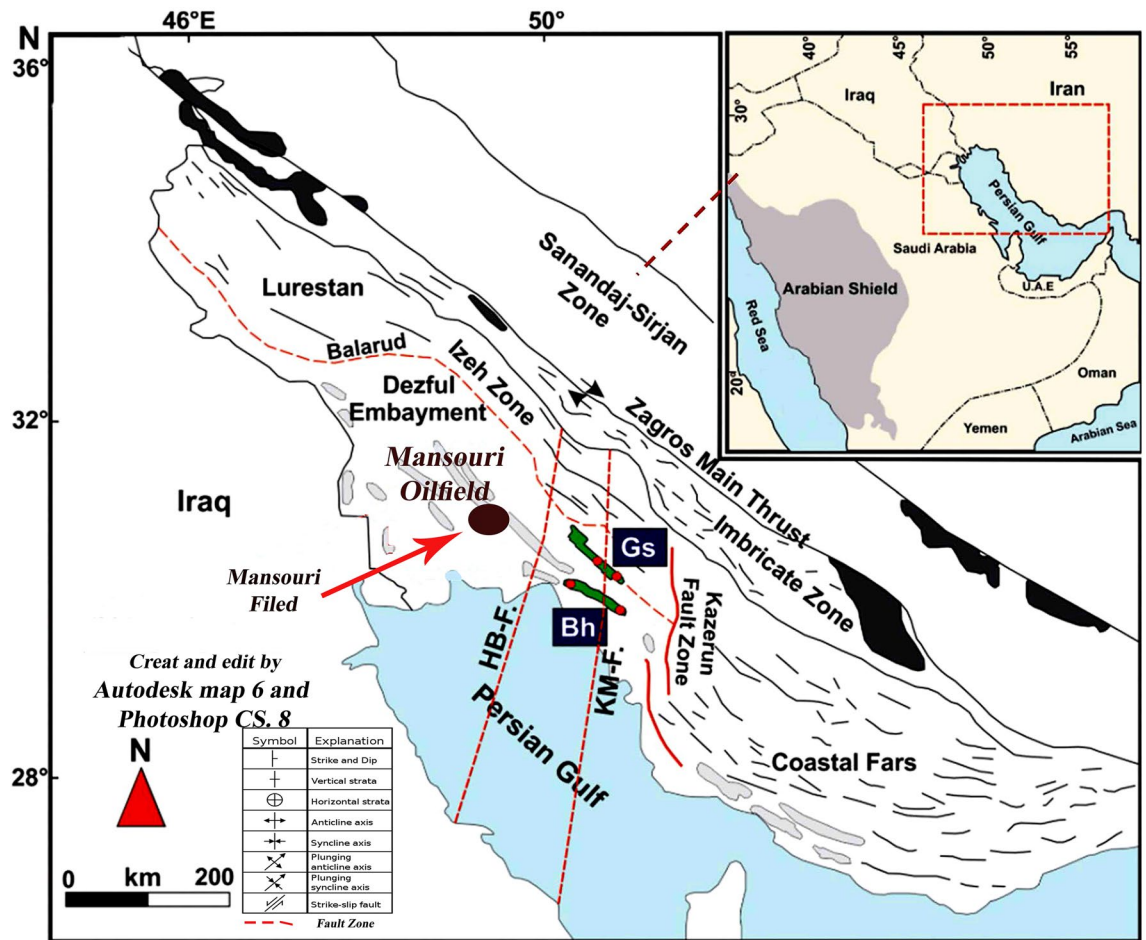
In Ilam Formation, the dominant lithology is White wackestone–mudstone, Brown packstone–wackestone, and White to brown limestone and argillaceous in some layers.

In Sarvak Formation, the dominant lithology is brown wackestone–packstone with dolomitization in upper intervals and dense limestone with asphaltic material in lower intervals.

In the bottom of the last zone, a gradational variation from the Kazhdumi shale to Sarvak limestone indicates a regressive environmental condition. The porosity data variation indicated that the reservoir quality would improve from the base to the top<sup>12,28,52,55</sup>.

## Methodology

Electrofacies (electrical facies) are identified using petrophysical logs such as gamma ray, resistivity, acoustic, density, and neutron. Since logs measure rocks' physical characteristics, electrofacies can be attributed to one or more lithofacies. Determination of facies is one of the main components of oil exploration and determination of reservoir properties<sup>28,30</sup>.



**Figure 1.** Location of Mansouri oilfield in the Dezful embayment, SW of Iran (create and edit by Autodesk Map 6)<sup>6,21,50</sup>.

### Estimating the number of distinct electrofacies

Due to electrofacies being determined experimentally, the number of different electrofacies is relatively incidental. The number of proper electrofacies is partially conditional to the number of log properties employed in their calculation and the joint nature of the statistical distributions of the log measurements. It also reflects the intention of electrofacies classification and the technique for assessing and employing the final classification. A simple recognition between reservoir and non-reservoir rock may be completed with an electrofacies classification of only two classes. At the same time, an investigation for environmental interpretation may demand a dozen or more classes<sup>5-7</sup>.

Due to a restricted number of well-logs that measure different physical effects in the employed well here, a proper electrofacies interpretation will only involve a few facies classes. Determining the proper number needs trial and error, beginning with many classes and lessening the number to eliminate trivial categories that contain only a few rare observations or combining ill-defined classes with comparable properties. The exact trial-and-error process can be utilized to assess alternative approaches like additional clustering algorithms<sup>3,42</sup>.

The pursuit of cluster analysis is to divide the data set into specific groups based on the similarity or differences between the groups. The data in each group have the most similarity and differences from those in other groups. The usual method for identifying and separating different sedimentary facies is to study thin sections prepared from core samples. However, the problem is the need for sufficient information on cores in the reservoir area. This information is available only in a very limited number of cored wells. One geological concern is preparing and explaining the sedimentary model with this limited information<sup>5,13-15,49</sup>. This study created an electric facies model utilizing a clustering method and well logs in a drilled well with coring in the Asmari Formation. Then it was compared with different clustering methods to get the best model, and then it was adjusted and improved with the facies obtained from the cored well logs and finally implemented in all the wells. In this regard, instead of the limited and unique information of a few cored wells, complete information on the simulated sedimentary facies was obtained in all the field wells, which significantly helped the sedimentary modeling of the studied field. In this research, MRGC and ANN clustering methods are used to determine electrical facies, which will be discussed in the following:

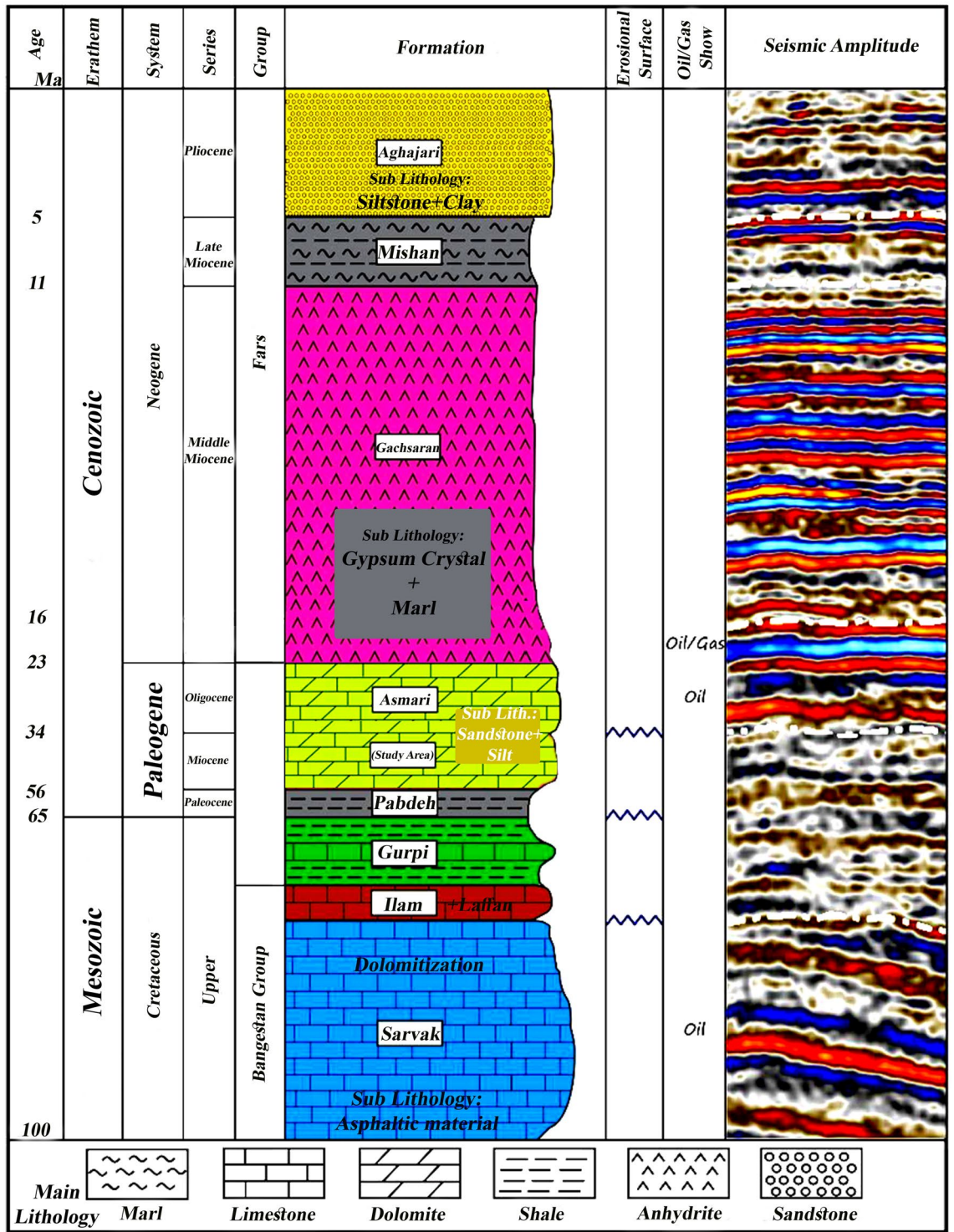
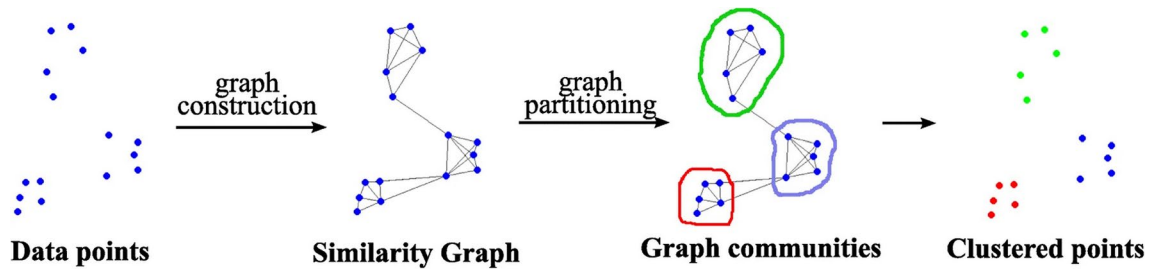


Figure 2. General stratigraphic column of Masouri oilfield with depicting study area<sup>12</sup>.

### MRGC clustering method

MRGC is one of the few non-parametric and very suitable methods for studying and analyzing data clusters obtained from well logs and drilling cores. This method has several benefits, such as the capability to identify natural patterns in the logs, no need for prior knowledge about the data, an automatic suggestion of the best number of clusters, the lowest parameters and insensitivity to their changes, and no restrictions on the type and number of data and clusters<sup>5,12,34,42</sup>. Schematic diagram of the workflow for multi graph-based clustering is presented in Fig. 3.



**Figure 3.** Multi graph-based data clustering via multiscale community detection<sup>5,6</sup>.

The data underlying structure is examined, and natural data groups that could have dissimilar shapes, sizes, densities, and relative separations are formed. MRGC defines the optimal number of clusters automatically, and the level of EF clusters can be specified based on actual requirements. It has a stable outcome and can efficiently partition the EF and indicate the LF from the well-log data. This approach involves the following two parameters to make the MRGC method more robust than other hierarchical clustering algorithms. Neighboring Index (NI) is a parameter based on the weighted rank of measurement point  $x$  relative to all other measurement points  $y$ . Two points close to each other can be easily separated if they have a high  $NI(x)$ . Subsequently, the number of facies can be easily specified using the Eqs. (1) to (4)<sup>6,18,34,42</sup>.

$$s(x) = \sum_{n=1}^{N-1} \exp(-m/\alpha) \quad (1)$$

$$s_{\min} = \min_{i=1,N} \{s(x_i)\} \quad (2)$$

$$s_{\max} = \max_{i=1,N} \{s(x_i)\} \quad (3)$$

$$NI(x) = \frac{s(x) - s_{\min}}{s_{\max} - s_{\min}} \quad (4)$$

where  $N$  is the total number of data points,  $x$  is the  $m_{th}$  nearest neighbor of  $y$  ( $m \leq N-1$ ), and  $\alpha$  is the smoothing parameter greater than zero.  $NI(x)$  varies from 0 to 1, and as the value of  $NI(x)$  increases, the point becomes closer to the kernel of a cluster.

Kernel representative index (KRI) is a parameter that combines  $NI(x)$ , the neighbor function  $M(x, y)$ , and the distance function  $D(x, y)$ . The factor  $NI(x)$  allows us to recognize the kernel of a cluster. The number of neighbors  $M(x, y)$  tends to generate clusters of equivalent size and clusters of equivalent volume from the distance  $D(x, y)$ . Combining these two factors produces a sufficient balance between a cluster's size and volume and generates consistent outcomes. KRI is estimated by employing the Eq. (5)<sup>1,6,34,42</sup>.

$$KRI(x) = NI(x) \cdot M(x, y) \cdot D(x, y) \quad (5)$$

where  $M(x, y) = m$ , when  $y$  is the  $m_{th}$  neighbor of  $x$ , and  $D(x, y)$  is the  $x$  and  $y$  distance.

First, the kernel points that influence all their neighboring data points (call members) are specified, and subsequently, all members are compared. The members affected by the kernel point affected the other members as well. Boundaries are assigned when a member is affected by its previous member but without affecting others. The NI of each point in the data set is calculated to identify the clusters. Subsequently, small natural groups of the points are formed based on the NI to determine a KNN attraction for each point. Independently, an optimal number of clusters is computed based on the KRI. Eventually, the terminal clusters are constructed by merging the small clusters<sup>1,5,6,9,18,26,34,42</sup>.

To determine the electrofacies with this method, first in the FACIMAGE™ section of the Geolog software, among the petrophysical logs, those logs that are most related to the results target, which include: gamma ray log (CGR), sonic log (DT), density log (RHOB), neutron log (NPFI) and water saturation (SW), is selected.

Data clustering is the basis of modeling and classification algorithms. This process aims to define small natural and essential groups from a large data group<sup>27,40</sup>. The MRGC method uses two indices NI (neighborhood index parameter) which determines the proximity of each point in a data set to the peak or trough of the probability density function of the data, and KRI (Kernel Representative Index), is an index used to determine points prone to represent the core or center of the cluster.

Define the neighborhood characteristic of any graph  $G$  without isolated vertices to be Eq. (6):

$$n.Char(G) = s_1 - s_2 + s_3 - \dots, \quad (6)$$

where:  $s_i$  is the number of subsets of  $V(G)$  of cardinality  $i$  that are externally dominated, meaning that  $S \subseteq N(v)$  for some  $v \in V(G) - S$ . Thus  $s_1 = n$  is just the order of  $G$ , and  $s_2$  is the number of pairs of vertices that have a common neighbor.

The neighborhood characteristic of a graph can also be calculated in terms of the complete bipartite subgraphs present in  $G$ . For every graph  $G$  without isolated vertices Eq. (7):

$$n.Char(G) = 2 \sum_{1 \leq i \leq j} (-1)^{i+j} k_{i,j} \tag{7}$$

where:  $k_{i,j}$  count the number of complete bipartite<sup>5,56</sup>.

Kernel functions allow mapping non-linearly separable points into a (generally) higher dimensional feature space so that the inner product in the new space can be computed without needing to compute the exact feature maps bringing further computational benefits. Although most algorithms in the broader field of machine learning have been developed for the linear case, real-world data often requires nonlinear models capable of unveiling the underlying complex relationships towards improving the performance of downstream tasks<sup>5,8,34,57</sup>. To use kernel functions for learning node representations via matrix factorization:

Let  $(X, d_x)$  be a metric space and  $H$  be a Hilbert space of real-valued functions defined on  $X$ . A Hilbert space is called reproducing kernel Hilbert space (RKHS) if the point evaluation map over  $H$  is a continuous linear functional. Furthermore, a feature map is defined as a function  $\Phi : X \rightarrow H$  from the input space  $X$  into feature space  $H$ . Every feature map defines a kernel  $K : X \times X \rightarrow R$  as follows (Eq. (8))<sup>8,57</sup>:

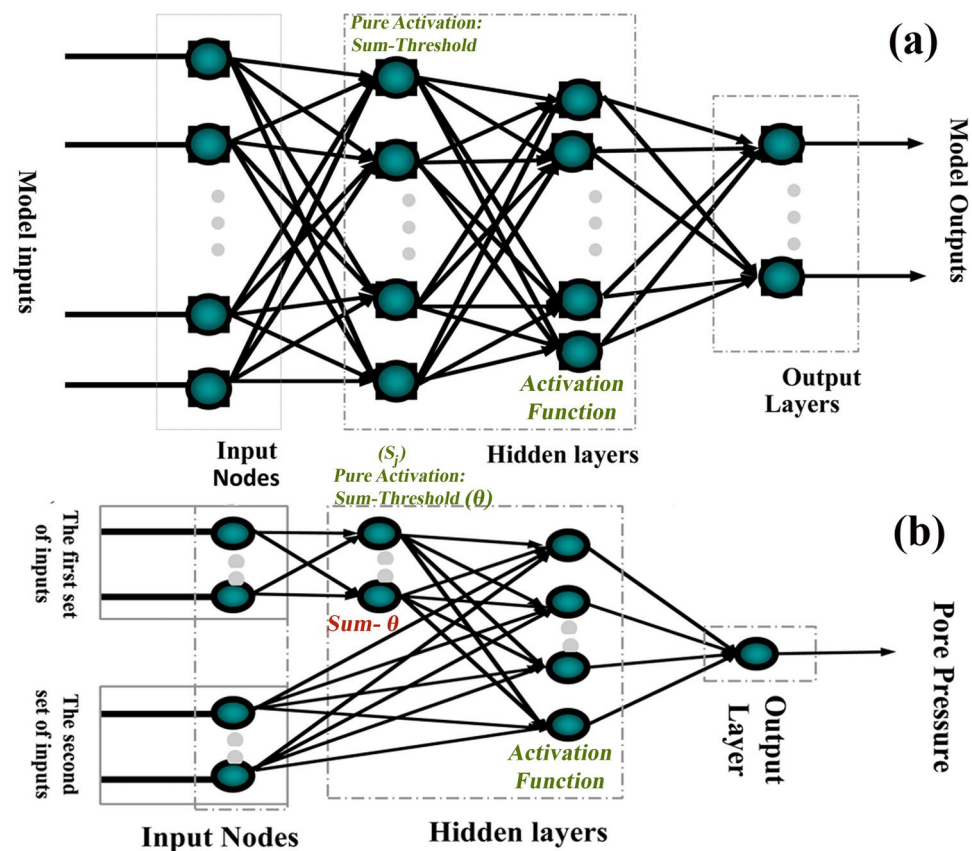
$$K(x, y) = (\Phi(x), \Phi(y)) \tag{8}$$

$$\forall(x, y) \in X^2$$

It can be seen that  $K(x, y)$  is symmetric and positive definite due to the properties of an inner product space<sup>5,8,57</sup>.

### Artificial neural networks (ANN) clustering method

A new method for determining electrical facies is applying artificial neural networks. The method teaches the network to produce a specific output based on the input data. Here, the network is trained using different algorithms. The network's training uses inputs whose output is also applied to the program. The trained network can now produce the desired output for new inputs. Each neural network has at least three layers (Fig. 4a). These layers include input, output, and intermediate (hidden) layers. Each input has its weight and enters the hidden layer using the combination function. The simplest mode of the combination layer is multiplying each input by



**Figure 4.** (a) Structure or topology of a typical forward neural network, (b) FFBPANN structure made by “Lianbo Hu” to predict pore pressure<sup>43,59</sup>.

weight and summing these numbers. This number is transferred to the output layer using the transfer function in the hidden layer. Some percent of the data are also used for comparison<sup>7,9,44,47,58,59</sup>.

The network node or artificial neuron acts as the biological neuron, and the connection weight of the neural network functions as the chemical transmitter and the electrical transmitter. ANN can intelligently analyze with simple mathematical methods and deal with nonlinear, fuzzy, and complex relationships. A neuron is the main element of an ANN, the model. The function of artificial neurons, as the name implies, is to simulate biological neurons. The artificial neuron has a P input and an output<sup>44,59</sup>.

The inputs are  $x_i$  ( $i = 1, \dots, p$ ), and the output is  $y_j$ . The relationship between inputs and outputs can be set as follows (Eq. (9)):

$$\begin{cases} S_j = \sum_{i=1}^p w_{ij} \cdot x_i - \theta_j \\ y_j = f(S_j) \end{cases} \quad (9)$$

Here  $\theta$  is the threshold.  $W_{ij}$  is the weight or weight of the connection from signal  $i$  to neuron  $j$ .  $S_j$  is pure activation, and  $f(S_j)$  is the activation function<sup>43,58</sup>. There are many activation functions, including linear, ramp, threshold, crushing, etc. Neurons are arranged in different ways depending on the type of network.

There are several types of connections or weighted links in neural networks:

- Forward: Most links are of this type in which the signals move in only one direction. There is no feedback (loop) from input to output. The output of each layer does not affect the same layer.
- Backward: Data is fed back from the nodes of the upper layer to the nodes of the lower layer.
- Lateral: The output of the nodes of each layer is used as the input of the nodes of the same layer.

The Feed-Forward Back Propagation Artificial Neural Network (FFBPANN) is widely used in petroleum engineering applications. The structure or topology of the feed-forward neural network is shown in Fig. 4b<sup>32,34,58,59</sup>.

The number of neurons significantly affects the prediction results; in the studied well, the Feed Forward-Backpropagation (FFBP-ANN) model based on the Lianbo Hu ANN method, the best combination of neurons is 2-5-1 format. It means that the first layer has two neurons, the second layer has five neurons, and the output layer has one neuron. Supplementary data are presented as an appendix at the end of the manuscript.

## Results

In the sequence of oil/gas wells, zoning is one operation that segregates the sequence studied into zones with common conditions (geological or reservoir conditions, etc.). This section used log data to represent the Asmari Formation in the Mansouri Field accurately. Zones with typical reservoir geology (lithology) are studied in the well sequences using read diagrams. Figure 5 shows the sequence of the study well after zoning.

After evaluating the sequence of the Asmari Formation, the petrophysical parameters are averaged to determine the best production intervals in terms of oil accumulation in the well, and the best intervals with the highest hydrocarbon volume are determined. The net production zone is an essential indicator in evaluating reservoir quality. This thickness comprises a part of the reservoir with acceptable reservoir and petrophysical conditions. Shear limits are determined to achieve this goal for some of the calculated petrophysical parameters. These intervals are the zones where the focus of the reservoir studies is concentrated. Based on zonation in wells, the cost and technology for cutting boundaries differed.

The shear boundaries for the carbonate and sandstone sequences of the Asmari Formation are presented in Table 1.

The cut of sandstone and carbonate values are determined from prepared well logs and calculating shale volume, saturation of water, porosity percent, and oil volume. More details of the calculations for each zone are presented in Table 2.

### Stratigraphy of the studied field

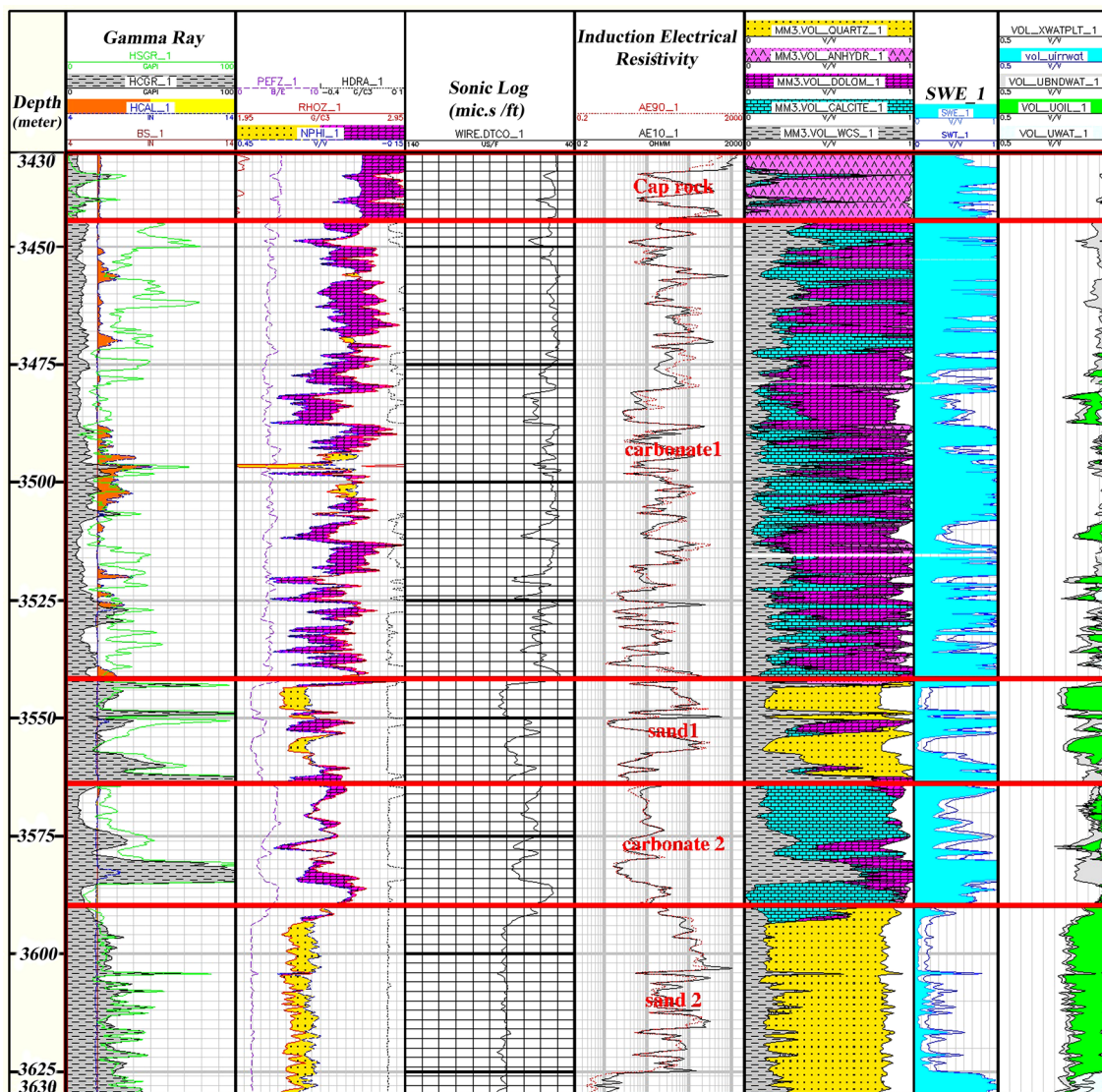
In the data preparation stage, after loading the data into the software, their quality in terms of readings, well control conditions, and logs used is checked. Afterward, the pre-computational stage is performed using well information, which finally obtained information about the well conditions and drilling mud properties in the evaluated sequence. Then environmental correction of the data is performed, and the effects of wells, drilling mud, etc., are removed from the logs readings, and consequently, zoning is performed using charts. In the next step, the lithology is evaluated and estimated in each sequence using corrected and edited logs and lithology cross-sections (neutron-density, Rho-U plot, MID plot, and MN plot). Finally, employing the probabilistic method, the petrophysical parameters are calculated in the whole sequence, and the average of these parameters is calculated in the whole well and each zone. The production zones are also identified in the wells studied using the average petrophysical parameters and determining the cutoff for some of these parameters.

In the sequence of oil/gas wells, zoning is one procedure that segregates the sequence studied into zones with common conditions (geological or reservoir conditions, etc.). This section used log data to represent the Asmari Formation in the Mansouri Field accurately. Zones with typical reservoir geology (lithology) are studied in the well sequences using read diagrams.

Based on petrophysical results, the Asmari Formation has been divided into five zones (Fig. 5).

Zone 1 (3444.5–3427.5 m): This zone exists in all drilled wells. The central part of the zone consists of dolomite plus a thick layer of limestone. Limestones are mostly cream to light brown and cream to gray, semi-hard to hard, fine-grained, micro-crystalline with anhydrite, chert, mudstone argillic to packstone (Fig. 6).





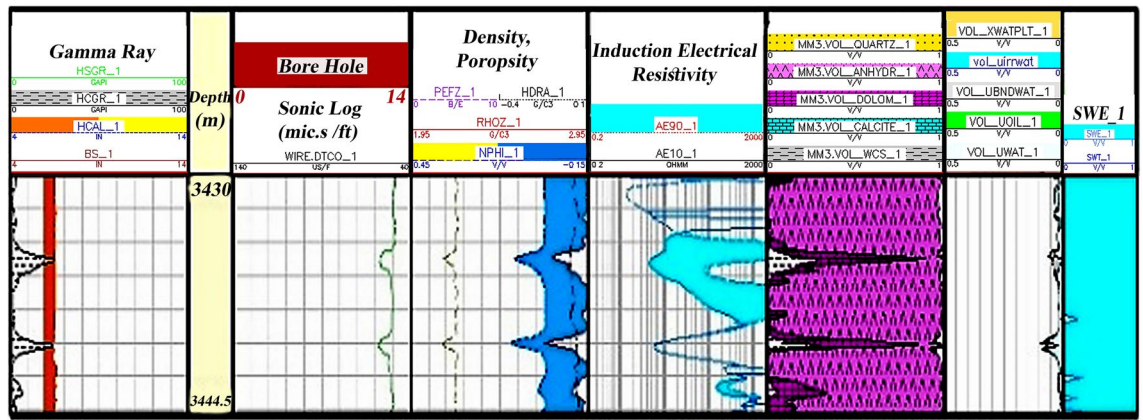
**Figure 5.** Reservoir zonation sequences of the Asmari Formation based on lithological alteration in the studied well.

Parameter	Type	Cut off (%) Carbonate	Cut off (%) Sandstone
PHIE	≥	4.5	8
SWE	≤	50	50
Vsh	≤	20	30

**Table 1.** Cutting off limits for carbonate and sandstone sections employing shale volume, water saturation, porosity and oil volume.

Interval (m)	Zone	Vsh (%)	PHIE (%)	SWE (%)	Uoil (%)
3427.5 to 3444.5	Zone-1	2.7	2.4	99	0.01
3444.5 to 3560.5	Zone-2	18.1	3.9	91.8	0.055
3560.5 to 3570.5	Zone-3	27.4	13.1	46.5	7.4
3570.5 to 3585	Zone-4	11.5	8.9	76.7	2.9
3585 to 3630	Zone-5	29.5	12.9	63	6.3

**Table 2.** Average petrophysical parameters calculated per weight for different zones in the Asmari Formation.



**Figure 6.** Initial petrophysical assessment based on lithology zoning segmentation 1.

Zone 2 (3560.5–3444.5 m): This zone is present in all wells. The lithology of this zone mainly consists of dolomite and sandstone (Fig. 7).

Zone 3 (3570.5–3560.5 m): Its dominant lithology includes shale, limestone, and sandstone (Fig. 8).

Zone 4 (3585–3570.5 m): This zone exists in all wells, and most of it contains a barrier/ beach ridge and is likely to be associated with the Ahwaz sand dunes. Much of the lithology of this zone is sandstone and shale (Fig. 9).

Zone 5 (3630–3585 m): This zone cannot be identified in all wells due to a lack of logging data. The main lithologies in this zone are shale, sandstone, and limestone (Fig. 10).

### Zoning

According to stratigraphical and petrophysical results, the segmentation zone 1 is 14.3 m thick in the well sequence. The dominant lithology of this zone is mainly anhydrite. A small percentage of shale and dolomite is also found in this zone. Due to the petrophysical property of anhydrite, this zone plays no role in the Asmari Formation in the well-studied. It has very low porosity and almost no hydrocarbon accumulation in this zone (Fig. 6).

According to Fig. 7, second zone, which has the most sequence in the studied well, is 116 m thick and has the dominant lithology of calcite and dolomite. At some intervals, there are pores in the zone with little oil accumulation. The average porosity in this zone is also low and has high water saturation and, consequently, low oil volume.

The third segment in Fig. 8 has a minimum thickness of about 10 m from the study well. It has good oil accumulation capacity with sand and shale lithology. The high porosity, and low water saturation with good hydrocarbon volume, make this zone the main reservoir zones in the studied well sequenced.

The lithological conditions in of fourth segment and zone (Fig. 9) are approximately the same as those of the second zone, with the dominant lithology being calcite and dolomite containing shale and anhydrite. Its thickness is 15 m. This zone has little porosity, and the water saturation is somewhat high, resulting in small quantities of oil.

Fifth zone occupies the last part of the Asmari Formation sequence in the studied well (Fig. 10) and is the main reservoir zone in the studied sequence. The lithology of this zone is similar to that of the 3rd zone, sand and shale zones, which have high porosity, low water saturation, and consequently higher oil accumulations than other zones. The zone is 45 m thick.

The average calculated petrophysical parameters of studied zones employing well-A are shown in Table 2. According to the information presented in this table, it can be seen that the average petrophysical parameters in zones 3 and 5 have the best reservoir conditions compared to other zones. Due to the consequence of these two zones, the main reservoir zones in the Asmari Formation sequence are studied in shaley sandstone lithology.

As depicted in Table 2, the shale volumes in zones 3 and 5 are 27.4% and 29.4%, respectively. Furthermore, porosities are 13.1% and 12.9%, water saturations are 46.5% and 63%, and oil volumes are 7.4% and 6.3% respectively. These facts show the clear distinction between these two zones and other zones in terms of the reservoir capacity of sandstone and shale in them. The following will discuss clustering methods to study electrofacies and compare them with lithofacies.

### Determination of electrical facies

The facies are categorized using appropriate electrical log readings and proper clustering methods. The total sedimentary units with lithological features, sedimentary structure, geometrical form, fossil appendages, longitudinal flow patterns, and similar layering surfaces are distinguishable from the characteristics mentioned above by facies<sup>38,60</sup>. Well logs are one of the primary sources of subsurface information in oil/gas fields. These tools exhibit features such as mineralogical composition, texture, sedimentary structures, and reservoir properties (such as porosity and permeability) directly or indirectly<sup>35,36</sup>. Nowadays, determining electrical facies in reservoir formations is one of the standard studies in the characterization of reservoirs. The wide use of these facies and their flexibility to determine specific reservoir parameters due to the type of input data has today made this method one of the most potent tools in reservoir studies. Facies data are used in cases such as separating reservoir zones

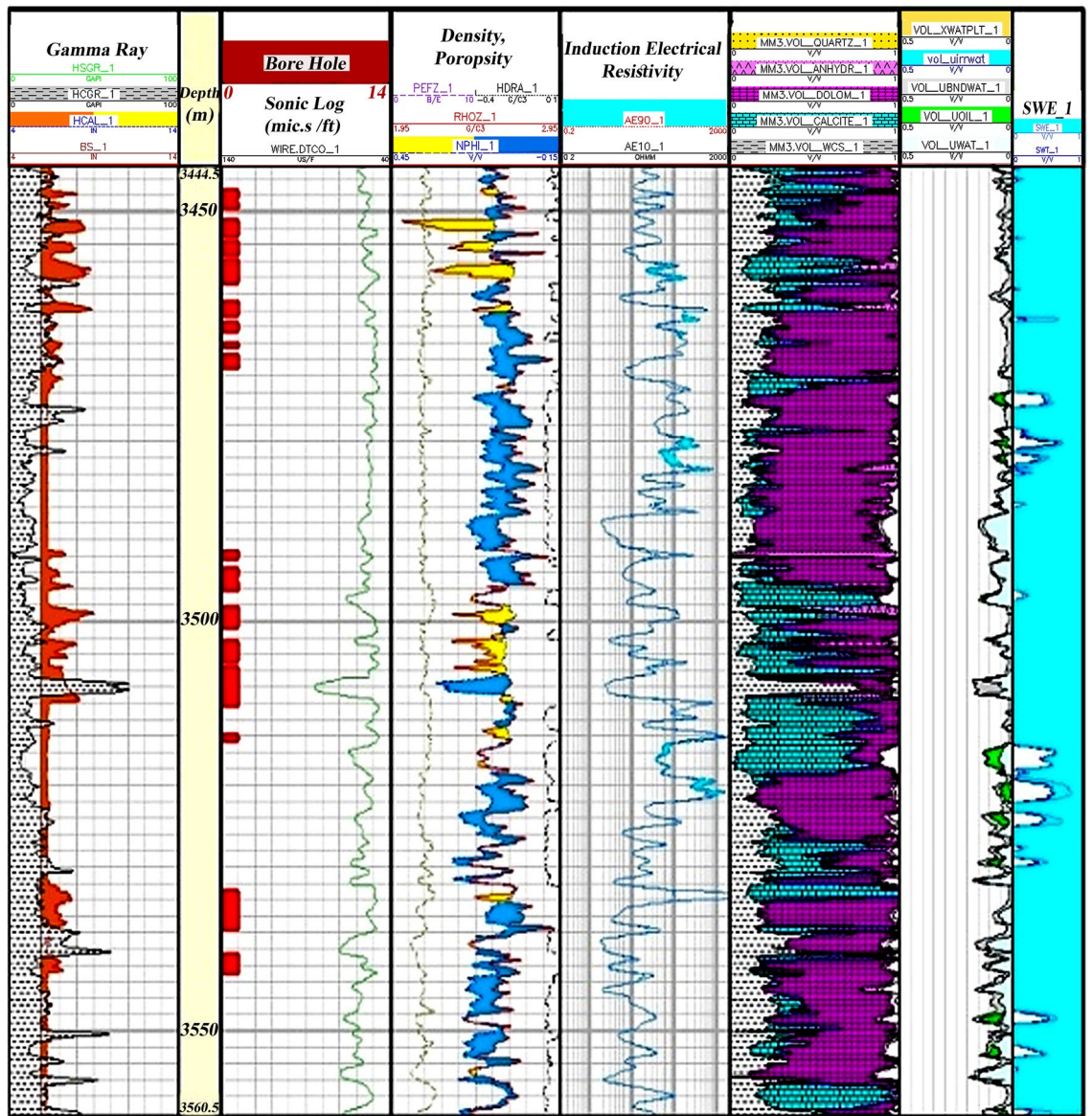


Figure 7. Initial petrophysical assessment based on lithology zoning segmentation 2.

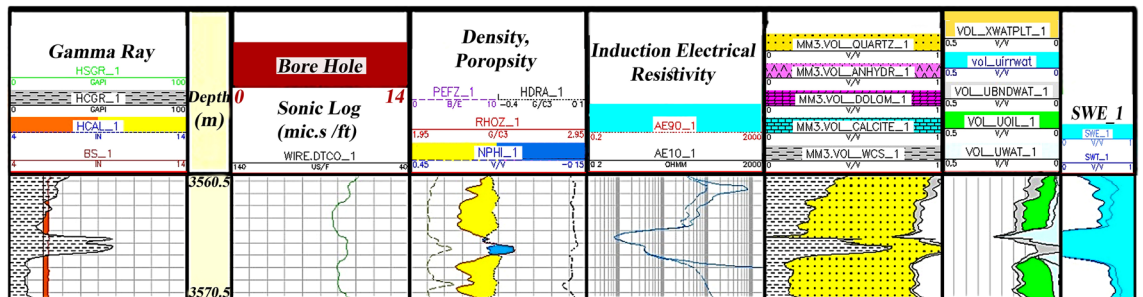


Figure 8. Initial petrophysical assessment based on lithology zoning segmentation 3.

from non-reservoir and in field-scale and large-scale structural adaptation. This data's importance is called the virtual core<sup>8,18,50</sup>.

In this study, facies with common geological/reservoir properties are classified into different categories using readings of gamma, neutron, density, acoustic, and resistivity diagrams. Figures 11 and 12 show the frequency diagrams of the input logs of the model and cross diagrams of these logs, respectively.

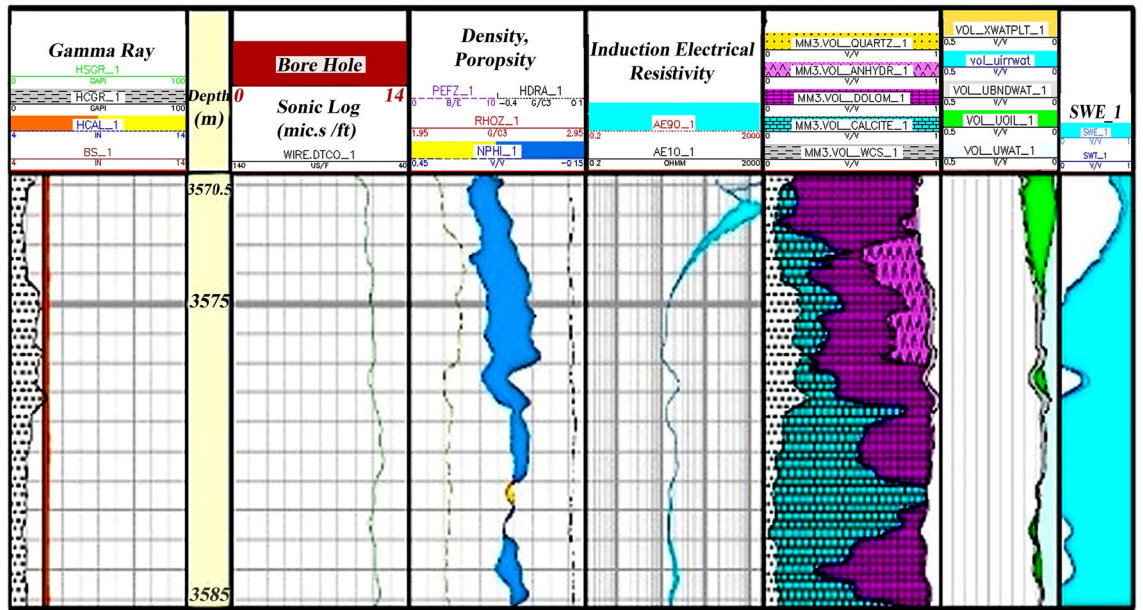


Figure 9. Initial petrophysical assessment based on lithology zoning segmentation 4.

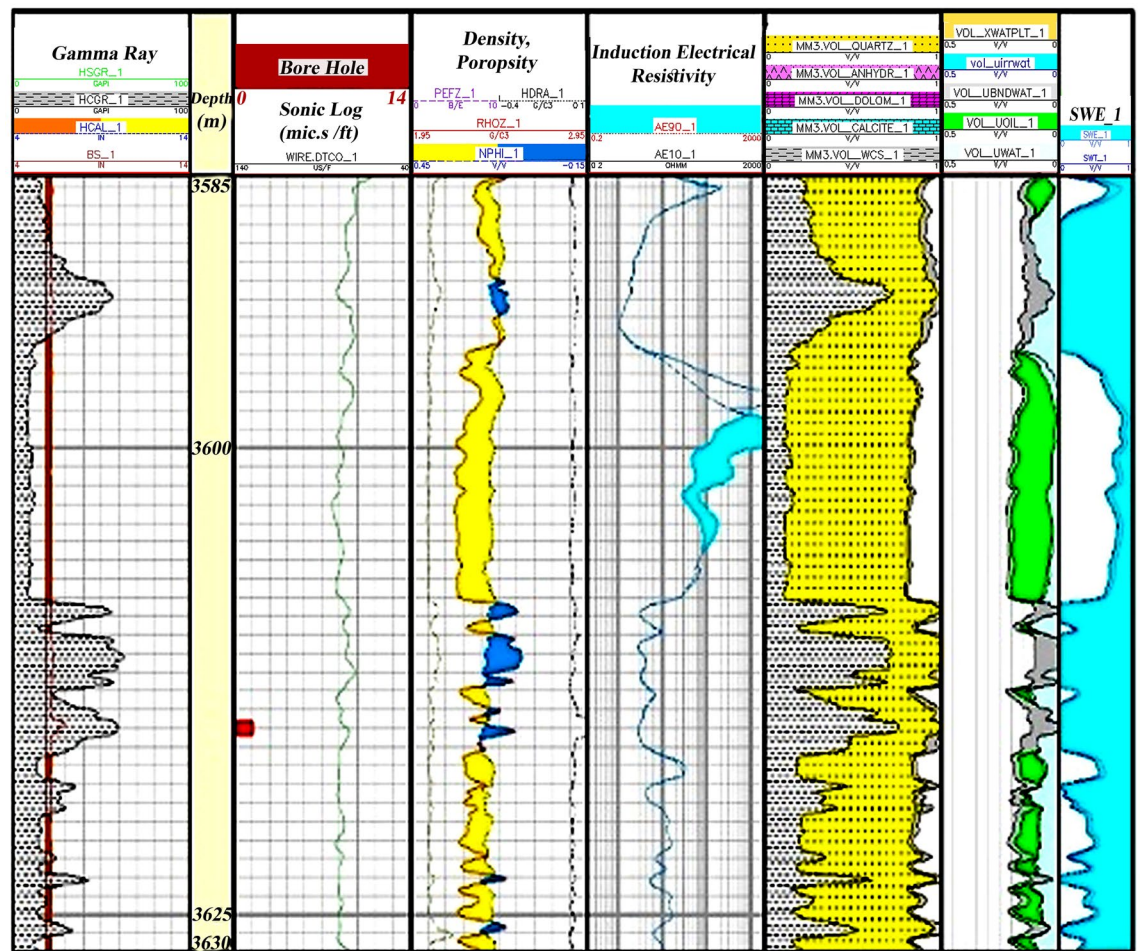


Figure 10. Initial petrophysical assessment based on lithology zoning segmentation 5.

### Model Logs

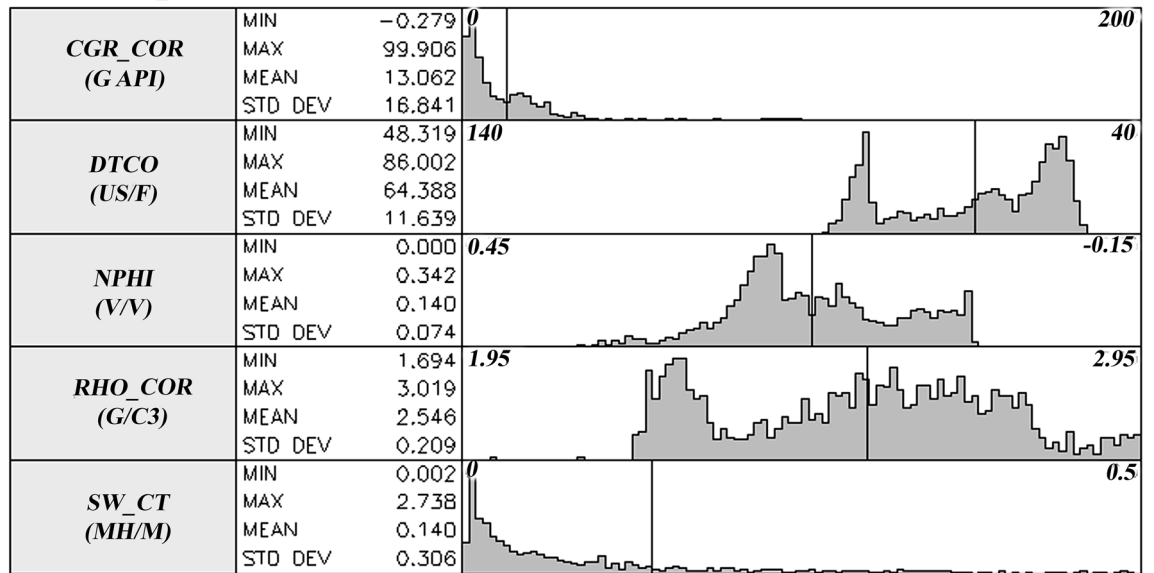


Figure 11. Frequency diagram of model input logs.

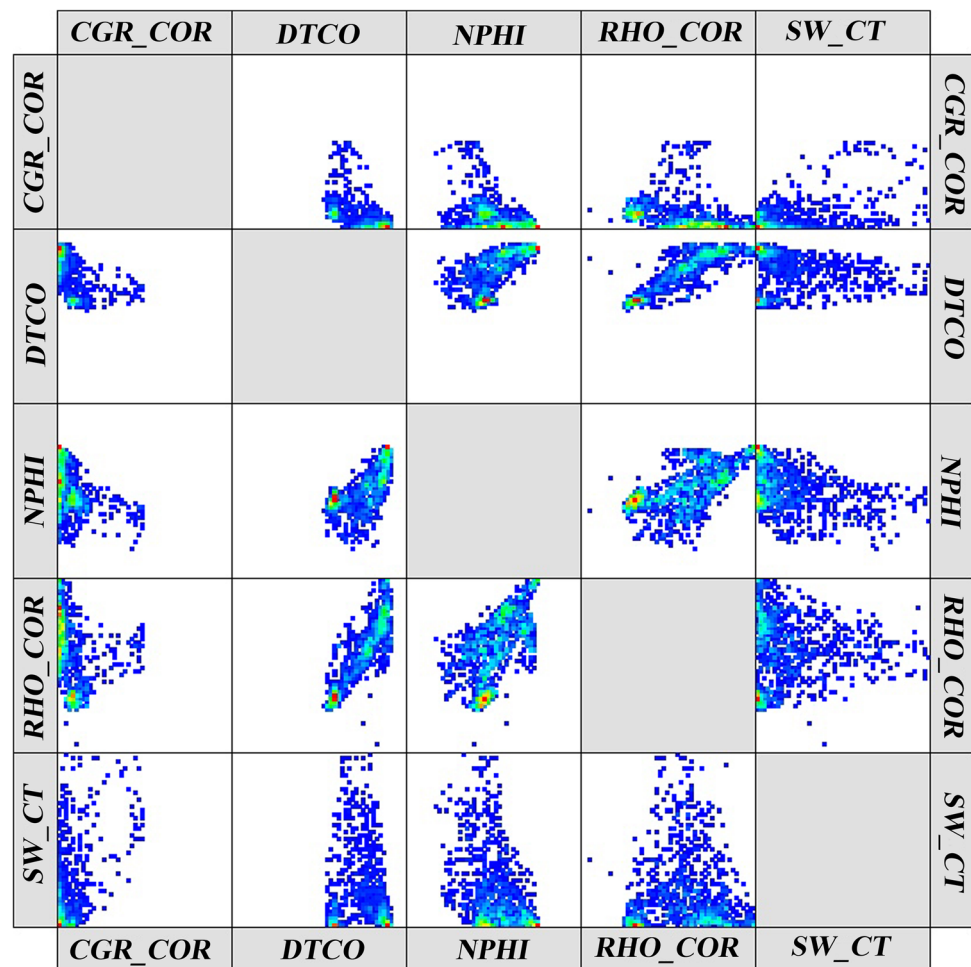


Figure 12. Cross-over diagram of model input logs relative to each other.

## Discussion

### MRGC clustering description

Data clustering is the basis of modeling and classification algorithms. This process aims to define small natural and fundamental groups of large datasets<sup>50,60</sup>. The MRGC (Multi-resolution graph-based clustering) method is one of the few non-parametric and very suitable methods for studying and analyzing data clusters from the logs with the characteristics mentioned. In this method, the log data is indexed by two NI (Neighboring Index Parameter) that determine the position of the proximity of each point in a dataset to the summit or probability of the density function of the data and the KRI (Kernel Representative Index) is an indicator to determine the prone points to represent the core or center of the cluster.

In this study, based on the MRGC clustering method, the upper and lower limit of optimal data and models are determined. Finally, applying this model produced an optimal model with eight facies. The results of categorized facies are presented in Fig. 13. It has shown the readings of each model input log in the separated facies with their weight.

Figure 14 shows the facies classification throughout the sequence of the Asmari Formation in the studied wells in the Mansouri Field. Furthermore, it has compared the lithofacies produced by the lithological column and the saturated and hydrocarbon columns. Comparing lithological columns in sandstone and carbonate lithologies and facies columns is clearly illustrated.

### ANN clustering description

An artificial neural network is a computerized model that attempts to emulate biological learning processes and simulate specific tasks of the human nervous system. Neurons are composed of neurons as microprocessors, each of which has a simple task. Based on the ANN clustering method, the present study assumed eight optimal facies in the previous stage to estimate an entire facies in the well by constructing an ANN model between petrophysical logs and the pre-facies logs. In constructing the neural network model, the Levenberg–Marquardt (L-M) algorithm trained the data. This network has three layers (input, hidden, and output). The number of neurons is calculated through trial and error and response optimization as 2-5-1. The facies classification throughout the sequence of the Asmari Formation is shown in Fig. 15.

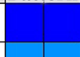
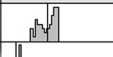
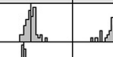

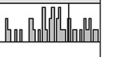

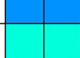

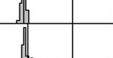
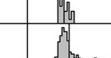


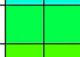

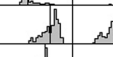
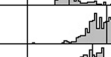
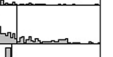

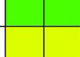
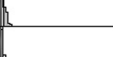




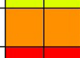
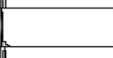
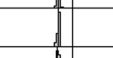

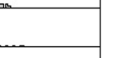




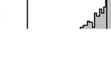


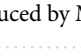
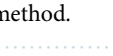




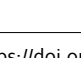
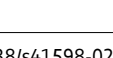
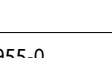



Figure 16 shows the correlation and comparing zoning results of all three Geolog, MRGC, and ANN clustering techniques. However, the number of MRGC and ANN's electrical facies classifications and lithofacies of the Geolog is different; similar results of correct separating of anhydrite, limestone, and sandstone are noticed, especially in zones three and five with dominant sandstone lithology.

### Geological lithofacies validating data

Based on previous microfacies studies, four sedimentary environments of open sea, dam, lagoon and coastal environment can be distinguished for the deposition of the Asmari Formation in this field, which is deposited on a platform with a low slope<sup>18,24,29</sup>. In this study, thin sections of the Asmari Formation in the studied well-A have identified 11 general facies. Asmari formation in the Mansouri field has clastic and carbonate components. Therefore, examining existing thin sections has led to the identification of two general facies: carbonate-evaporitic facies and siliceous-clastic petrofacies. In order to validate the results, the siliceous petrofacies data is used with the assumption that the electrofacies are not necessarily related to the lithofacies and that different facies can be placed inside a specific clustering zone. Siliceous-clastic petrofacies are describes as:

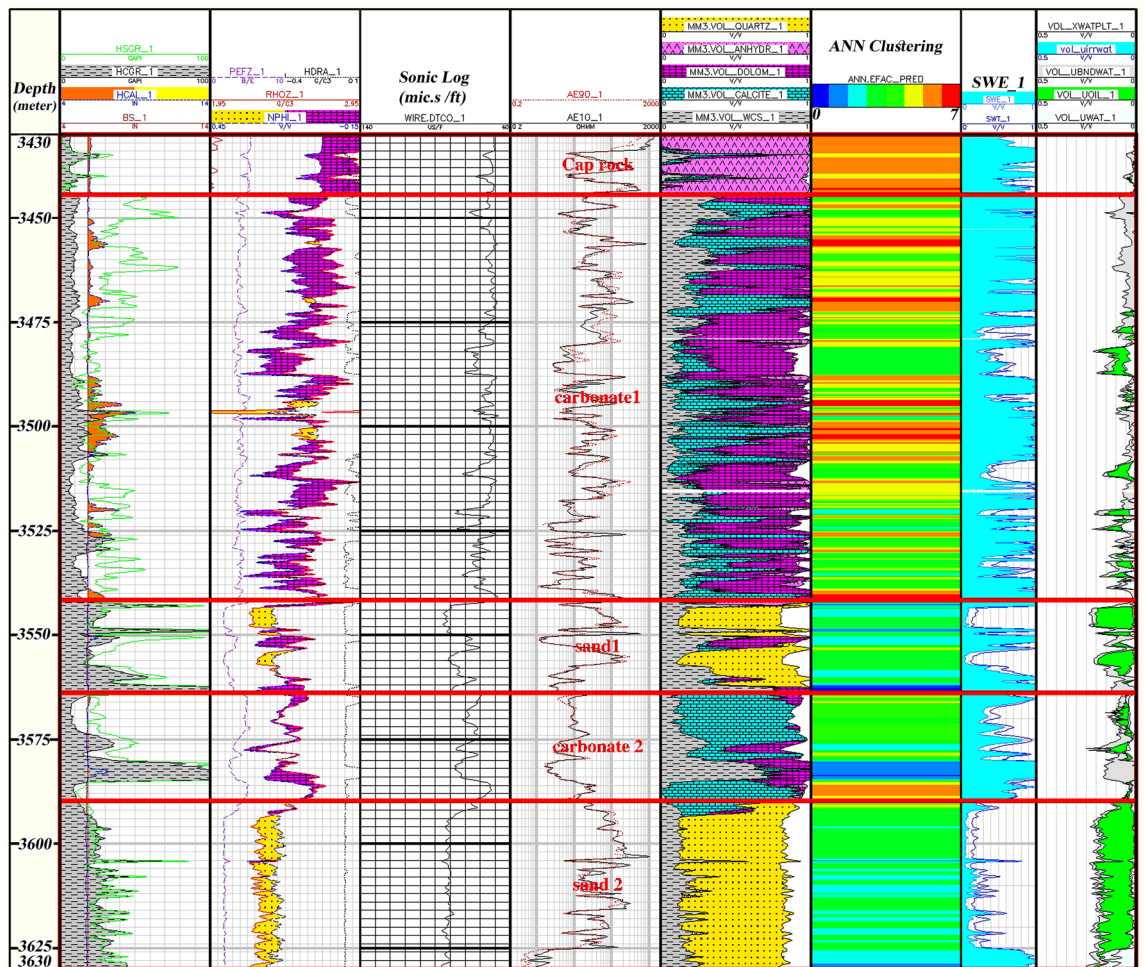
### Quartz arenite petrofacies

This microfacies contains more than 95% quartz. Quartz particles are often angular and have suitable welding. In this field, sandstones are usually seen in two ways: (a) loose sand, where no cement can be seen between the quaternary particles. (b) Sandstones with carbonate or sulfate cement, carbonate cement often includes dolomite and sometimes micrite limestone, and sulfate cement also includes anhydrite. Due to the texture maturity and appropriate particle melting, these facies can be attributed to a coastal environment with high energy (Fig. 17a and b).

	Name	Color Pattern	Weight	CGR_COR	DTCO	NPHI	RHO_COR	SW_CT
1	FACIES_1		51					
2	FACIES_2		30					
3	FACIES_3		350					
4	FACIES_4		435					
5	FACIES_5		138					
6	FACIES_6		53					
7	FACIES_7		83					
8	FACIES_8		172					

**Figure 13.** Facies produced by MRGC method.





**Figure 15.** Classification of facies in the well sequence and final evaluation results using the ANN method.

for three parameters of effective porosity, effective water saturation, and shale volume. After applying these shear zones, the potential zones with high oil accumulation are identified.

- Petrophysical parameter facts depict the clear distinction between zones 3 and 5 in terms of the reservoir capacity of sandstone and shale.
- Regarding estimating electrical facies by MRGC and ANN methods, despite the differences in concepts and methods, these techniques are all exclusively powerful tools for predicting electrical facies.
- In addition, the results show that intelligent systems can successfully model patterns in test data when there is a logical relationship between input data or between input and output data. The model can be used for Recognition and making reasonable conclusions between actual and estimated data. Suppose the parameters necessary for making these models are adjusted, regardless of the lithology and formation characteristics in the relevant oilfield. In that case, these methods can also be applied to other field wells that lack specific facies.
- On the other hand, by comparing the performance of the parameters measured and estimated from different methods, it can be concluded that the MRGC method is more accurate and successful than other methods for determining these parameters in the wells.
- In conclusion, it is worth noting that MRGC is an efficient method for clustering and homogenizing data and determining different reservoir parameters, which, in addition to the high speed of operation, is not limited to data size and numbers.
- Comparing MRGC and ANN electrofacies and lithofacies demonstrate similar results of correct separating of anhydrite, limestone, and sandstone are noticed, especially in zones three and five with dominant sandstone lithology
- The siliceous petrofacies from describing thin sections are employed for data validation with the assumption that the electrofacies are not necessarily related to the lithofacies and that different facies can be placed inside a specific clustering zone. Accordingly, most of the facies that exist in zone 3 and 5 depths include sandstone and dolomite facies show comparable results with MRGC and ANN electrofacies.

It is suggested to considering core data from nearby wells in the Asmari Formation to more accurately evaluate and check the accuracy of rock type determination utilizing flow zone index (FZI) and fuzzy center mean



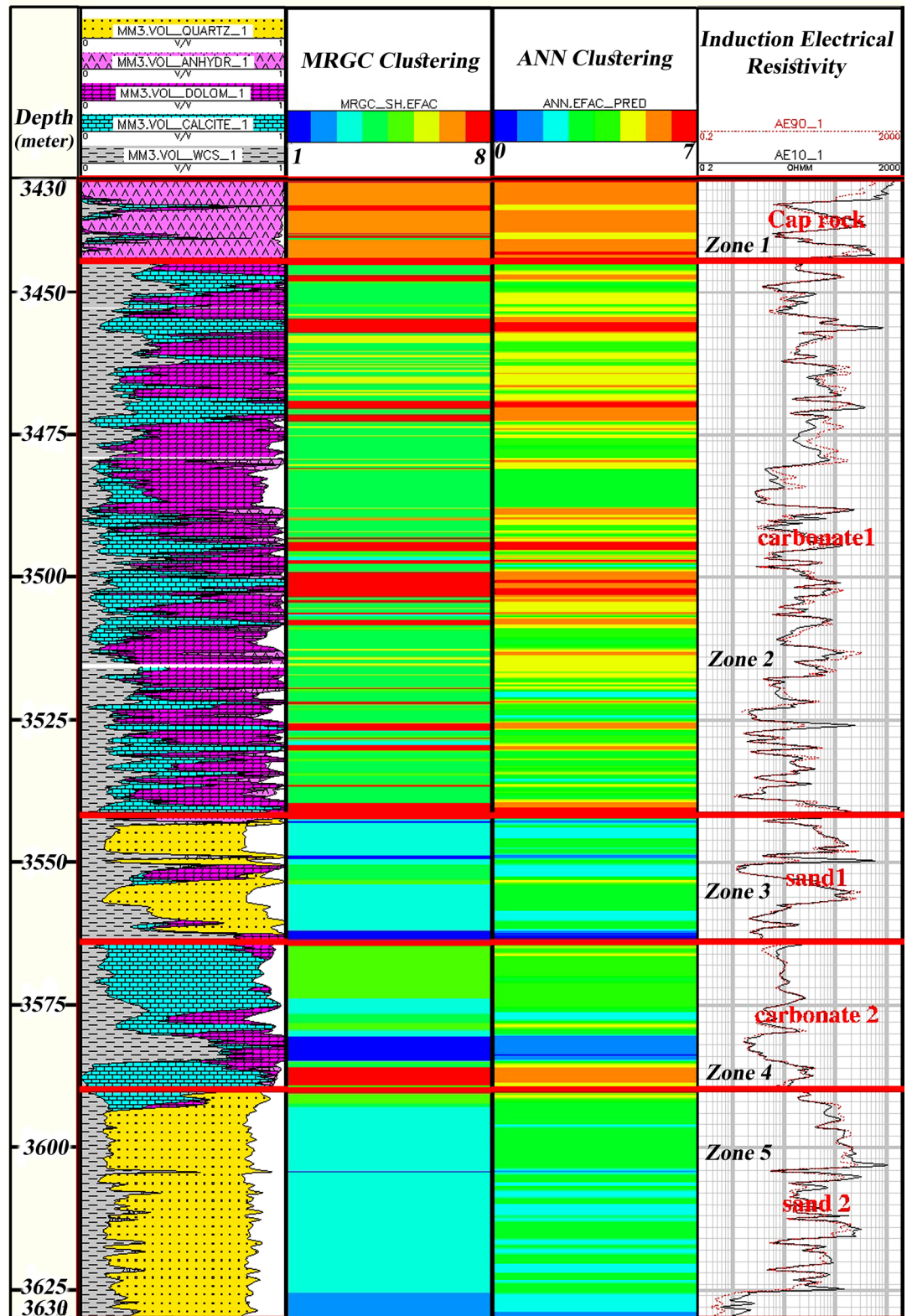
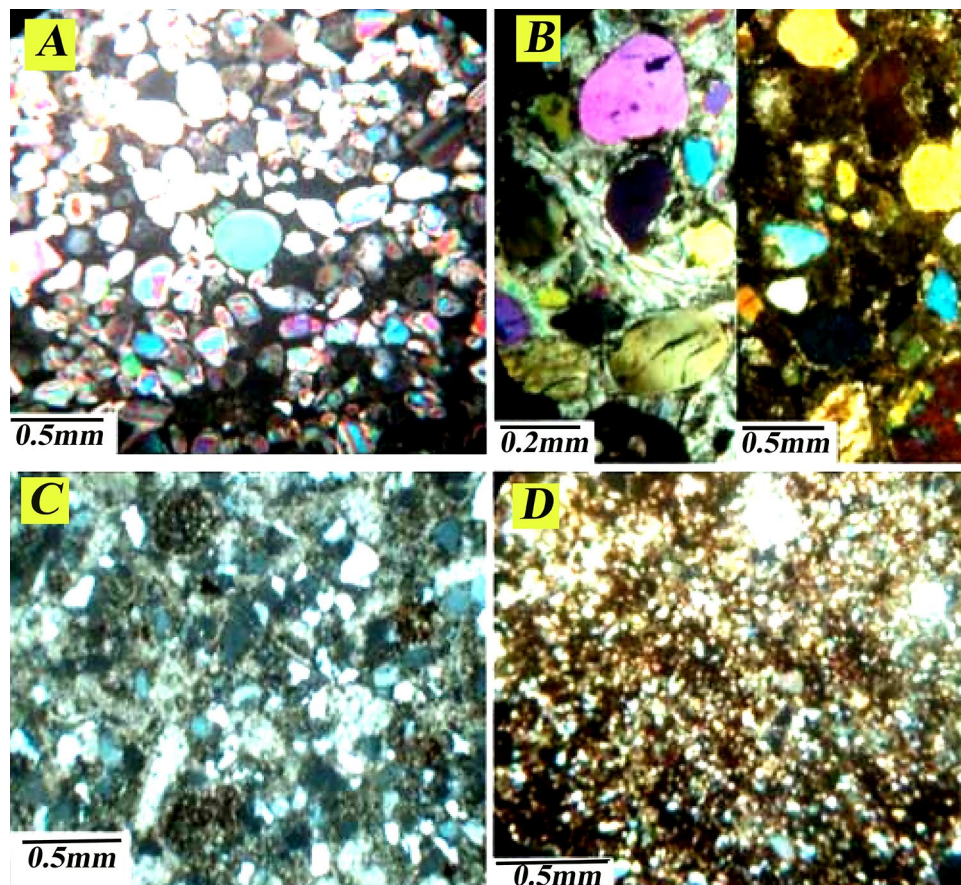
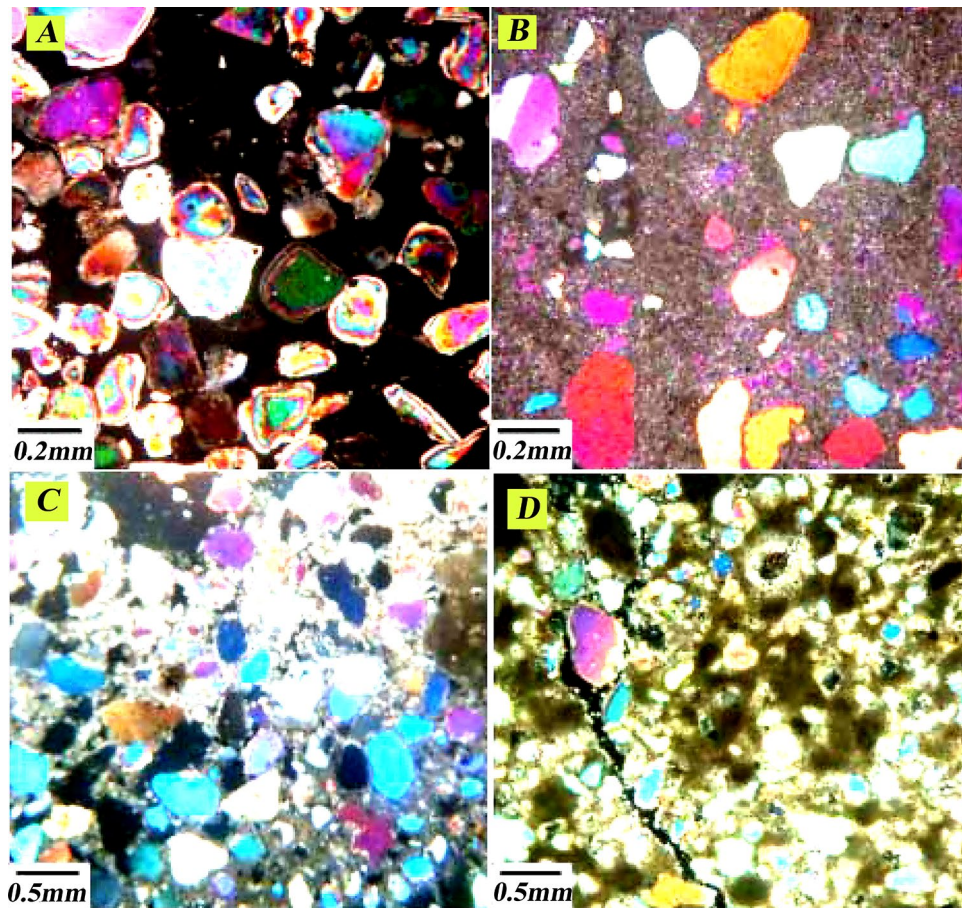


Figure 16. Comparing zoning results of the Geolog, MRGC, and ANN clustering techniques in the Asmari Formation.



**Figure 17.** (a) Quartz arenite microfacies without cement, (b) quartz arenite microfacies with sulfate and dolomite cement, (c) sublitharenite petrofacies, (d) siltstone petrofacies of Well No. A, Mansouri oilfield.

(FCM). Furthermore, it is possible to use MRGC and ANN clustering zone to determine sandstone reservoir in nearby drilled wells and generalize the results to coreless wells in the Asmari Formation of Mansouri oilfield (Supplementary Information).



**Figure 18.** Drilling sample thin sections of the Asmari Formation in Mansouri field includes (A) without cement sandstones due to migrating hydrocarbons before cementing, (B) dissolution in sandstones, (C) dolomite cement in sandstones, (D) dolomite dissolution in sandstones.

### Data availability

The following datasets generated and/or analyzed during the current study are available in the Mahmoud Memariani repository, <https://doi.org/10.13140/RG.2.2.19913.31847>. The other datasets generated and/or analyzed during the current study are not publicly available due to not permitted to share by National Iranian Oil Company Exploration Directorate (NIOC-EXP) request but are available from the corresponding author on reasonable request.

Received: 25 November 2023; Accepted: 29 February 2024

Published online: 02 March 2024

### References

- Shoghi, J., Bahramizadeh-Sajjadi, H., Nickandish, A. B. & Abbasi, M. Facies modeling of synchronous successions—A case study from the mid-Cretaceous of NW Zagros, Iran. *J. Afr. Earth Sci.* **162**, 103696. <https://doi.org/10.1016/j.jafrearsci.2019.103696> (2020).
- Kolbikova, E., Gusev, S., Malinovskaya, O., Garaev, A. & Valiev, R. Lithofacies analysis of Devonian carbonate deposits based on geological and geophysical information analysis by using machine learning methods. *Eur. Assoc. Geosci. Eng.* **2021**(1), 1–6. <https://doi.org/10.3997/2214-4609.202159047> (2021).
- Davis, J. C. Electrofacies in reservoir characterization. In *Handbook of Mathematical Geosciences: Fifty Years of IAMG* (eds Daya Sagar, B. S. *et al.*) 211–223 (Springer International Publishing, 2018). [https://doi.org/10.1007/978-3-319-78999-6\\_11](https://doi.org/10.1007/978-3-319-78999-6_11).
- Sabouhi, M. *et al.* Stratigraphic influences on reservoir heterogeneities of the Mid-Cretaceous carbonates in southwest Iran: Insight from an integrated stratigraphic, diagenetic and seismic attribute study. *J. Asian Earth Sci.* **243**, 105514. <https://doi.org/10.1016/j.jseaes.2022.105514> (2023).
- Mahadasu, P. & Singh, K. H. Electrofacies estimation of carbonate reservoir in the Scotian Offshore Basin, Canada using the multi-resolution graph-based clustering (MRGC) to develop the rock property models. *Arab. J. Sci. Eng.* <https://doi.org/10.1007/s13369-022-07521-x> (2022).
- Khazaie, E. *et al.* Electrofacies modeling as a powerful tool for evaluation of heterogeneities in carbonate reservoirs: A case from the Oligo-Miocene Asmari Formation (Dezful Embayment, southwest of Iran). *J. Afr. Earth Sc.* **195**, 104676. <https://doi.org/10.1016/j.jafrearsci.2022.104676> (2022).
- Al-Iessa, I. A. & Zhang, W. Z. Facies evaluation and sedimentary environments of the Yamama Formation in the Ratawi oil field, South Iraq. *Sci. Rep.* **13**(1), 5305. <https://doi.org/10.1038/s41598-023-32342-9> (2023).

8. Okhovvat, H. R., Riahi, M. A. & Akbari Dehkharghani, A. Kernel principal component analysis (KPCA) in electrical facies classification. *Iran. J. Oil Gas Sci. Technol.* <https://doi.org/10.22050/ijogst.2023.360469.1653> (2023).
9. Rastegarnia, M., Sanati, A. & Javani, D. A comparative study of 3D FZI and electrofacies modeling using seismic attribute analysis and neural network technique: A case study of Cheshmeh-Khosh Oil field in Iran. *Petroleum* **2**(3), 225–235. <https://doi.org/10.1016/j.petlm.2016.06.005> (2016).
10. Kianoush, P., Mohammadi, G., Hosseini, S. A., Khah, N. K. F. & Afzal, P. Compressional and shear interval velocity modeling to determine formation pressures in an oilfield of SW Iran. *J. Min. Environ.* **13**(3), 851–873. <https://doi.org/10.22044/jme.2022.12048.2201> (2022).
11. Ding, J.-W., Ma, H.-Y., Yang, Q.-S., Lu, Y. & Yin, S.-J. Study on logging identification method of complex lithology in X oilfield. (Paper presented at the Proceedings of the International Field Exploration and Development Conference 2021, Singapore) [https://doi.org/10.1007/978-981-19-2149-0\\_4](https://doi.org/10.1007/978-981-19-2149-0_4) (2022).
12. Soleimani, B., Moradi, M., Ghabeshavi, A. & Mousavi, A. Permeability variation modeling and reservoir heterogeneity of Bangestan carbonate sequence, Mansouri oilfield, SW Iran. *Carbonates Evaporites* **34**(1), 143–157. <https://doi.org/10.1007/s13146-018-0461-y> (2019).
13. Saleh, A. H., Hemimey, W. A. E. & Leila, M. Integrated geological and petrophysical approaches for characterizing the pre-nomanian Nubian sandstone reservoirs in Ramadan Oil Field, Central Gulf of Suez, Egypt. *Arab. J. Sci. Eng.* **48**(6), 7939–7958. <https://doi.org/10.1007/s13369-023-07743-7> (2023).
14. Opuwari, M. *et al.* Petrophysical core-based zonation of OW oilfield in the Bredasdorp Basin South Africa. *Sci. Rep.* **12**(1), 510. <https://doi.org/10.1038/s41598-021-04447-6> (2022).
15. Esfandyari, M., Mohseni, H. & Heidari, M. Facies analysis, depositional sequences and platform evolution of the Sarvak Formation (late Albian-Turonian) in the Zagros Basin, West of Iran. *J. Afr. Earth Sci.* **198**, 104811. <https://doi.org/10.1016/j.jafrearsci.2022.104811> (2023).
16. Rafik, B. & Kamel, B. Prediction of permeability and porosity from well log data using the nonparametric regression with multivariate analysis and neural network, Hassi R'Mel Field, Algeria. *Egypt. J. Pet.* **26**(3), 763–778. <https://doi.org/10.1016/j.ejpe.2016.10.013> (2017).
17. Radwan, A. E. Modeling the depositional environment of the sandstone reservoir in the middle Miocene Sidri Member, Badri Field, Gulf of Suez Basin, Egypt: Integration of gamma-ray log patterns and petrographic characteristics of lithology. *Nat. Resour. Res.* **30**(1), 431–449. <https://doi.org/10.1007/s11053-020-09757-6> (2021).
18. Jafarzadeh, N., Kadkhodaie, A., Ahmad, B. J., Kadkhodaie, R. & Karimi, M. Identification of electrical and petrophysical rock types based on core and well logs: Utilizing the results to delineate prolific zones in deep water sandy packages from the Shah Deniz gas field in the south Caspian Sea basin. *J. Nat. Gas Sci. Eng.* **69**, 102923. <https://doi.org/10.1016/j.jngse.2019.102923> (2019).
19. Kelkar, M. Exploitation and optimization of reservoir performance in Hunton formation, Oklahoma. 190. <https://doi.org/10.2172/815450> (U.S. Department of Energy, Assistant Secretary for Fossil Energy, 2005).
20. Sherkati, S. & Letouzey, J. Variation of structural style and basin evolution in the central Zagros (Izeh zone and Dezful Embayment), Iran. *Mar. Pet. Geol.* **21**(5), 535–554. <https://doi.org/10.1016/j.marpetgeo.2004.01.007> (2004).
21. Noorian, Y. *et al.* Control of climate, sea-level fluctuations and tectonics on the pervasive dolomitization and porosity evolution of the Oligo-Miocene Asmari Formation (Dezful Embayment, SW Iran). *Sediment. Geol.* **427**, 106048. <https://doi.org/10.1016/j.sedgeo.2021.106048> (2022).
22. Lai, J. *et al.* Typical misinterpretations and scientific concepts in well-logging geologic studies. *Nat. Gas Ind. B* **10**(2), 198–211. <https://doi.org/10.1016/j.ngib.2023.02.003> (2023).
23. Ismail, M. J., Ettensohn, F. R., Handhal, A. M. & Al-Abadi, A. Facies analysis of the Middle Cretaceous Mishrif Formation in southern Iraq borehole image logs and core thin-sections as a tool. *Mar. Pet. Geol.* **133**, 105324. <https://doi.org/10.1016/j.marpetgeo.2021.105324> (2021).
24. AbdollahieFard, I., Sherkati, S., McClay, K. & Haq, B.U. Chapter 2—Tectono-sedimentary evolution of the Iranian Zagros in a global context and its impact on petroleum habitats. In *Developments in Structural Geology and Tectonics*, Vol. 3 (ed. Saekin, A. F.) 17–28. <https://doi.org/10.1016/B978-0-12-815048-1.00002-0> (Elsevier, 2019).
25. Senosy, A. H., Ewida, H. F., Soliman, H. A. & Ebraheem, M. O. Petrophysical analysis of well logs data for identification and characterization of the main reservoir of Al Baraka Oil Field, Komombo Basin, Upper Egypt. *SN Appl. Sci.* **2**(7), 1293. <https://doi.org/10.1007/s42452-020-3100-x> (2020).
26. Kiaei, H., Sharghi, Y., Ilkhchi, A. K. & Naderi, M. 3D modeling of reservoir electrofacies using integration clustering and geostatistic method in central field of Persian Gulf. *J. Pet. Sci. Eng.* **135**, 152–160. <https://doi.org/10.1016/j.petrol.2015.08.019> (2015).
27. Kadkhodaie, A. & Kadkhodaie, R. A review of reservoir rock typing methods in carbonate reservoirs: Relation between geological, seismic, and reservoir rock types. *Iran. J. Oil Gas Sci. Technol.* **7**(4), 13–35. <https://doi.org/10.22050/ijogst.2019.136243.1461> (2018).
28. Abdideh, M. & Ameri, A. Cluster analysis of petrophysical and geological parameters for separating the electrofacies of a gas carbonate reservoir sequence. *Nat. Resour. Res.* **29**(3), 1843–1856. <https://doi.org/10.1007/s11053-019-09533-1> (2020).
29. Talaie, F., Kadkhodaie, A., Arian, M. & Aleali, M. Geochemical assessment of upper Cretaceous crude oils from the Iranian part of the Persian Gulf Basin: Implications for thermal maturity, potential source rocks, and depositional setting. *Pet. Res.* <https://doi.org/10.1016/j.ptlrs.2023.01.002> (2023).
30. Tavoosi Iraj, P., Rajabi, M. & Ranjbar-Karami, R. Integrated petrophysical and heterogeneity assessment of the Karstified Fahliyan formation in the Abadan Plain, Iran. *Nat. Resour. Res.* **32**(3), 1067–1092. <https://doi.org/10.1007/s11053-023-10175-7> (2023).
31. Jouini, S., Umbhauer, F., Leduc, J.-P. & Keskes, N. Petrophysical properties prediction using 3D core scanner imagery (Paper Presented at the SPE Annual Technical Conference and Exhibition) <https://doi.org/10.2118/116393-ms> (2008).
32. Kianoush, P., Mohammadi, G., Hosseini, S. A., Khah, N. K. F. & Afzal, P. Inversion of seismic data to modeling the interval velocity in an oilfield of SW Iran. *Results Geophys. Sci.* **13**, 100051. <https://doi.org/10.1016/j.ringps.2023.100051> (2023).
33. Abraham-A, R. M., Tassinari, C. C. G., Taioli, F., Rocha, H. V. & da Silva, O. C. Reservoir quality evaluation as a measure to forecast hydrocarbon and CO<sub>2</sub> storage prospects in Irati and Rio Bonito Formations, Paraná Basin. *Results Geophys. Sci.* **14**, 100059. <https://doi.org/10.1016/j.ringps.2023.100059> (2023).
34. Wu, H. *et al.* Adaptive multi-resolution graph-based clustering algorithm for electrofacies analysis. *Appl. Geophys.* **17**(1), 13–25. <https://doi.org/10.1007/s11770-020-0806-x> (2020).
35. Serra, O. & Abbott, H. T. The contribution of logging data to sedimentology and stratigraphy. *Soc. Pet. Eng. J.* **22**(01), 117–131. <https://doi.org/10.2118/9270-pa> (1982).
36. Serra, O. *Fundamentals of well-log interpretation/O. Serra; translated from the French by Peter Westaway and Haydn Abbott*, <https://nla.gov.au/nla.cat-vn904133> (Elsevier; Elf Aquitaine, 1984).
37. Wolf, M. & Pelissier-Combesure, J. Faciolog—Automatic Electrofacies Determination (Paper Presented at the SPWLA 23rd Annual Logging Symposium). <https://onepetro.org/SPWLAALS/proceedings-abstract/SPWLA-1982/All-SPWLA-1982/SPWLA-1982-FF/18804> (1982).
38. Selley, R. C. *Ancient Sedimentary Environments: And Their Sub-surface Diagnosis* (Routledge, 1995). <https://doi.org/10.4324/9780203059845>.
39. Tavakkoli, V. & Amini, A. Application of multivariate cluster analysis in logfacies determination and reservoir zonation, case study of Marun Field, South of Iran. *J. Sci. Univ. Teheran* **32**(2), 69–75 (2006).

40. Gharachelou, S., Amini, A., Kadkhodaei, A., Hosseini, Z. & Honarmand, J. Rock typing and reservoir zonation based on the NMR logging and geological attributes in the mixed carbonate-siliciclastic Asmari Reservoir. *Geopersia* **8**(1), 77–98. <https://doi.org/10.22059/geope.2017.237140.648333> (2018).
41. El Sharawy, M. S. & Gaafar, G. R. Reservoir zonation based on statistical analyses: A case study of the Nubian sandstone, Gulf of Suez, Egypt. *J. Afr. Earth Sci.* **124**, 199–210. <https://doi.org/10.1016/j.jafrearsci.2016.09.021> (2016).
42. Tian, Y. *et al.* Multi-resolution graph-based clustering analysis for lithofacies identification from well log data: Case study of intra-platform bank gas fields, Amu Darya Basin. *Appl. Geophys.* **13**(4), 598–607. <https://doi.org/10.1007/s11770-016-0588-3> (2016).
43. Kianoush, P., Mohammadi, G., Hosseini, S. A., Keshavarz Faraj Khah, N. & Afzal, P. ANN-based estimation of pore pressure of hydrocarbon reservoirs—a case study. *Arab. J. Geosci.* **16**(5), 302. <https://doi.org/10.1007/s12517-023-11373-6> (2023).
44. Mohammadinia, F., Ranjbar, A., Kafi, M. & Keshavarz, R. Application of machine learning algorithms in classification of the flow units of the Kazhdumi reservoir in one of the oil fields in southwest of Iran. *J. Pet. Explor. Prod. Technol.* **13**(6), 1419–1434. <https://doi.org/10.1007/s13202-023-01618-1> (2023).
45. Alameedy, U. S., Almomen, A. T. & Abd, N. Evaluating machine learning techniques for carbonate formation permeability prediction using well log data. *Iraqi Geol. J.* <https://doi.org/10.46717/igj.56.1D.14ms-2023-4-23> (2023).
46. Masroor, M., Emami Niri, M. & Sharifinasab, M. H. A multiple-input deep residual convolutional neural network for reservoir permeability prediction. *Geoenergy Sci. Eng.* **222**, 211420. <https://doi.org/10.1016/j.geoen.2023.211420> (2023).
47. Kianoush, P. *Formation Pressure Modeling by Integration of Seismic Data and Well Information to Design Drilling Fluid. Case Study: Southern Azadegan Field.* Ph.D. Dissertation, Petroleum and Mining Engineering Department, Islamic Azad University, South Tehran Branch. 325, <https://doi.org/10.13140/RG.2.2.11042.20169> (2023).
48. Varkouhi, S. & Wells, J. The relation between temperature and silica benthic exchange rates and implications for near-seabed formation of diagenetic opal. *Results Geophys. Sci.* **1–4**, 100002. <https://doi.org/10.1016/j.ringps.2020.100002> (2020).
49. Fang, X. & Feng, H. Study on discriminant method of rock type for porous carbonate reservoirs based on Bayesian theory. *Sci. Rep.* **11**(1), 18622. <https://doi.org/10.1038/s41598-021-98154-x> (2021).
50. Mohammadian, E., Kheirollahi, M., Liu, B., Ostadhassan, M. & Sabet, M. A case study of petrophysical rock typing and permeability prediction using machine learning in a heterogenous carbonate reservoir in Iran. *Sci. Rep.* **12**(1), 4505. <https://doi.org/10.1038/s41598-022-08575-5> (2022).
51. Hosseini, S. A. *et al.* Boundaries determination in potential field anomaly utilizing analytical signal filtering and its vertical derivative in Qeshm Island SE Iran. *Results Geophys. Sci.* **14**, 100053. <https://doi.org/10.1016/j.ringps.2023.100053> (2023).
52. Kianoush, P., Mohammadi, G., Hosseini, S. A., Keshavarz Faraj Khah, N. & Afzal, P. Determining the drilling mud window by integration of geostatistics, intelligent, and conditional programming models in an oilfield of SW Iran. *J. Pet. Explor. Prod. Technol.* **13**(6), 1391–1418. <https://doi.org/10.1007/s13202-023-01613-6> (2023).
53. Hosseini, S. A. *et al.* Tilt angle filter effect on noise cancelation and structural edges detection in hydrocarbon sources in a gravitational potential field. *Results Geophys. Sci.* **14**, 100061. <https://doi.org/10.1016/j.ringps.2023.100061> (2023).
54. Hosseini, S. A. *et al.* Integration of fractal modeling and correspondence analysis reconnaissance for geochemically high-potential promising areas, NE Iran. *Results Geochem.* <https://doi.org/10.1016/j.ringeo.2023.100026> (2023).
55. Barach, B. A. B., Jaafar, M. Z., Gaafar, G. R., Agi, A. & Junin, R. Development and identification of petrophysical rock types for effective reservoir characterization: Case study of the Kristine Field, Offshore Sabah. *Nat. Resour. Res.* **30**(3), 2497–2511. <https://doi.org/10.1007/s11053-021-09851-3> (2021).
56. Rezaei, S., Eshrati, P. & Eshrati, D. Neighborhood definition: A comparison between residents' and experts' points of views case of study of a historical neighborhood in Kermanshah, Iran. *Int. J. Architect. Eng. Urban Plan.* **32**(4), 1–16. <https://doi.org/10.22068/ijaup.692> (2022).
57. Celikkanat, A., Shen, Y. & Malliaros, F. D. Multiple kernel representation learning on networks. *IEEE Trans. Knowl. Data Eng.* **35**(6), 6113–6125. <https://doi.org/10.1109/TKDE.2022.3172048> (2023).
58. Zhang, J., Hu, J. & Liu, J. Neural network with multiple connection weights. *Pattern Recogn.* **107**, 107481. <https://doi.org/10.1016/j.patcog.2020.107481> (2020).
59. Hu, L. *et al.* A new pore pressure prediction method-back propagation artificial neural network. *Electron. J. Geotech. Eng.* **18**, 4093–4107 (2013).
60. Rezvandehy, M., Leung, J. Y., Ren, W., Hollands, B. & Pan, G. An improved workflow for permeability estimation from image logs with uncertainty quantification. *Nat. Resour. Res.* **28**(3), 777–811. <https://doi.org/10.1007/s11053-018-9418-z> (2019).

## Acknowledgements

The authors consider it necessary to express their sincere gratitude to the esteemed experts of the Research Institute Petroleum Industry (RIPI) and Exploration Directorates of the National Iranian Oil Company (NIOC) for constructive comments to improve the article's scientific level.

## Author contributions

S.H.E. conceptualization, programming, analysis, writing, editing; M.M. Supervision, analysis; Z.M. Review and Editing, M.A. Supervision, editing, P.K. Review, editing, writing. All authors reviewed the manuscript.

## Competing interests

The authors declare no competing interests.

## Additional information

**Supplementary Information** The online version contains supplementary material available at <https://doi.org/10.1038/s41598-024-55955-0>.

**Correspondence** and requests for materials should be addressed to M.M.

**Reprints and permissions information** is available at [www.nature.com/reprints](http://www.nature.com/reprints).

**Publisher's note** Springer Nature remains neutral with regard to jurisdictional claims in published maps and institutional affiliations.



**Open Access** This article is licensed under a Creative Commons Attribution 4.0 International License, which permits use, sharing, adaptation, distribution and reproduction in any medium or format, as long as you give appropriate credit to the original author(s) and the source, provide a link to the Creative Commons licence, and indicate if changes were made. The images or other third party material in this article are included in the article's Creative Commons licence, unless indicated otherwise in a credit line to the material. If material is not included in the article's Creative Commons licence and your intended use is not permitted by statutory regulation or exceeds the permitted use, you will need to obtain permission directly from the copyright holder. To view a copy of this licence, visit <http://creativecommons.org/licenses/by/4.0/>.

© The Author(s) 2024